

Sassy Title

by

E. Ross



A thesis submitted to the
University of Birmingham
for the degree of
DOCTOR OF PHILOSOPHY

Solar and Stellar Physics Group (SASP)
School of Physics and Astronomy
University of Birmingham
Birmingham, B15 2TT
Month 20XX

Abstract

You're awesome. Make sure the examiners know it

Acknowledgements

Who do you hate least?

Contents

1 HiSPARC as a Space Weather Detector	1
1.1 Introduction	1
1.2 Aims	1
1.3 HiSPARC Properties	2
1.4 HiSPARC Observations	3
1.5 Air Shower Simulations	5
1.6 Standardisation of HiSPARC Data	9
2 HiSPARC Station 14008	13
2.1 Introduction	13
2.2 Aims	13
2.3 HiSPARC 14008 Detector Set-up	13
2.4 Calibration	13
2.5 Observations	13
2.6 Observations	13
2.7 Conclusions	13
Bibliography	13

List of Figures

1.1	Azimuthal and zenith variations in the allowed and forbidden trajectories for HiSPARC station 501 on January 20th 2005	2
1.2	HiSPARC data for stations 501 and 3001 around the epoch of GLE 70. The plot shows the minute-averaged and 5-minute-averaged trigger events between detectors within the station. The vertical red, dashed line depicts the approximate onset time of the GLE.	4
1.3	HiSPARC data for stations 8001 and 3001 around the epoch of GLE 71. The plot shows the minute-averaged and 5-minute-averaged trigger events between detectors within the station. The vertical red, dashed line depicts the approximate onset time of the GLE.	5
1.4	HiSPARC data for 4 stations around the epoch of GLE 72. The top panel of each subplot shows the minute-averaged trigger events between detectors within the station, while the bottom panel shows the mean-shifted, minute-averaged counts by each individual detector in the station. The vertical red, dashed line depicts the approximate onset time of the GLE.	6
1.5	HiSPARC data for stations 501 and 8001 around the epoch of the FD in March 2012. The plot shows the minute-averaged and hourly-averaged trigger events between detectors within the station. The vertical blue-dashed line shows the approximate onset-time of the FD.	8
1.6	HiSPARC data for stations 501 and 8001 around the epoch of the FD in July 2012. The plot shows the minute-averaged and hourly-averaged trigger events between detectors within the station. The vertical blue-dashed line shows the approximate onset-time of the FD.	8
1.7	HiSPARC data for 4 stations around the epoch of the FD in December 2014. The plot shows the minute-averaged and hourly-averaged trigger events between detectors within the station. The vertical blue-dashed line shows the approximate onset-time of the FD.	9
1.8	HiSPARC data for [n] stations around the epoch in which there were several FDs close to the onset of GLE 72. The top panel of each subplot shows the minute-averaged trigger events between detectors within the station, while the bottom panel shows the mean-shifted, minute-averaged counts by each individual detector in the station. The vertical blue-dashed lines show the approximate onset-times of the two FDs observed around this epoch and the red-dashed line depicts the approximate onset time of the GLE.	10

1.9	Mean muon density footprints for (a) proton-initiated air showers and (b) α -particle-initiated air showers with intial PCR trajectories with zenith angles $\theta = 0^\circ$ and various PCR energies. The error bars given represent 1σ	11
1.10	Mean number of muons produced at ground level by the PCR for (a) proton-initiated air showers and (b) α -particle-initiated air showers, for various PCR energy. The uncertainty bars given represent 1σ	11

List of Tables

1.1	Properties of some of the HiSPARC stations: geographic longitude (λ), geographic latitude (ϕ), altitude (h), and the geomagnetic vertical cut-off rigidity (R_C) calculated from the PLANETOCOSMICS simulations.	3
1.2	Space weather events investigated within the HiSPARC data. The percentage change column provides a reference of how much the CR counts observed by the NM station at Oulu ($R_c=0.81$ GV) increased or decreased by, due to the space weather event.	4
1.3	PCRs simulated using CORSIKA.	7

Structure of Thesis

Text on how thesis is structured. Also a statement of what work you did yourself.

This thesis is comprised of four analysis chapters in addition to an introduction and conclusion. These chapters cover five separate projects I have completed during my PhD. At the start of each chapter a detailed statement is given explaining the contribution of work by myself or collaborators for each project.

Chapters ?? and ?? have already been published (?) and ? respectively), where I am first author on both works. These chapters are reproductions of the published works, aside from minor formatting changes to comply with thesis regulations.

Chapter ?? is comprised of two separate works that share many analysis techniques. Both halves of the chapter are presented in a format commensurate with the structure of a paper. Two papers are in preparation and will be submitted soon. I shall be first and second author on these papers respectively.

Finally, Chapter ?? is also presented in a format similar to a paper, and is essentially a draft near to submission, that again I shall be first author on.

As some of the chapters are verbatim reproductions of published or works in preparation, there is a level of repetition between some of the introductory and analysis sections, in each chapter, and Chapter ??.

1 HiSPARC as a Space Weather Detector

1.1 Introduction

1.1.1 HiSPARC Project

1.1.2 HiSPARC Detector

- design
 - scintillators
 - typical layouts (i.e. 2d or 4d)
 - trigger conditions

1.2 Aims

The HiSPARC project was set up with the detection philosophy of observing extended air showers (EAS), which are typically associated with PCRs with energy of $\sim 10^{14}$ eV and above, that produce large footprints observable with many HiSPARC stations simultaneously. For PCRs with energy below $\sim 10^{14}$ eV the air shower is small, with almost no observable footprint, and for PCRs with energy below $\sim 10^{11}$ eV, there are typically less than one or two muons that reach the ground, making their observation difficult.

The HiSPARC detectors are capable of observing any muons that reach them, therefore the project was motivated by the existing network of muon detectors which may have the capability of observing the cosmic rays associated with space weather events.

The principle aim of the project was to determine whether the existing HiSPARC network is capable of observing space weather events. This was initially achieved by investigating the data during periods of space weather activity to search for the associated signatures. In addition, simulations of air showers initiated by CRs were conducted to understand the expected muon flux at ground level.

1.3 HiSPARC Properties

- Locations of stations - Rigidities - Asymptotic viewing directions

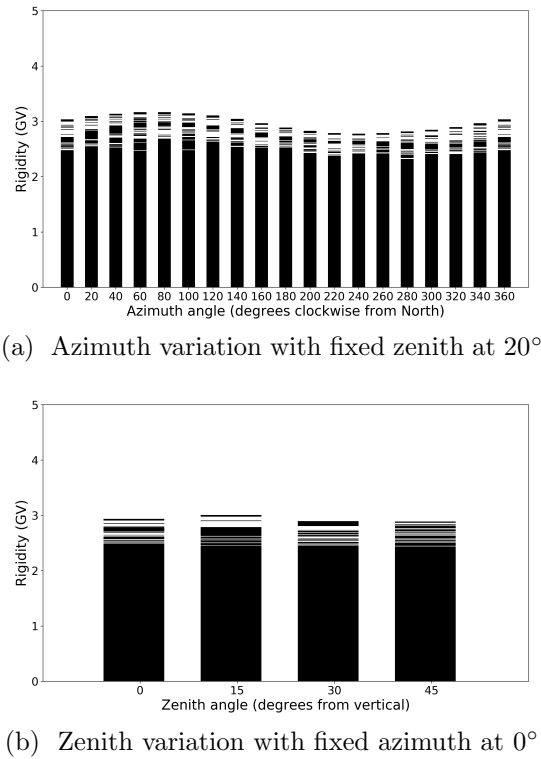


Figure 1.1: Azimuthal and zenith variations in the allowed and forbidden trajectories for HiSPARC station 501 on January 20th 2005

From the results of the PLANETOCOSMICS simulations it was possible to calculate the rigidity cut-off for each HiSPARC station using equation (??). The cut-off rigidity calculated for the six HiSPARC stations for a vertical incidence upon the atmosphere (i.e. 0° zenith angle) are shown in Table 1.1 which show that there is little variation in R_C between the HiSPARC stations and that they observe protons with rigidities in excess of ~ 3 GV.

Table 1.1: Properties of some of the HiSPARC stations: geographic longitude (λ), geographic latitude (ϕ), altitude (h), and the geomagnetic vertical cut-off rigidity (R_C) calculated from the PLANETOCOSMICS simulations.

Station Name/ID	R_C [GV]	λ [deg]	ϕ [deg]	h [m]	No. Detectors
Nikhef/501	3.19	4.95 E	52.36 N	56.18	4
College Hageveld/203	3.18	4.63 E	52.35 N	53.71	2
Leiden/3001	3.23	4.45 E	52.17 N	54.08	2
Eindhoven/8001	3.44	5.49 E	51.45 N	70.12	2
Birmingham University/14001	3.06	1.93 W	52.45 N	204.14	4

The small variation between HiSPARC stations is due to their close proximity in geographic latitude and longitude. The values of R_C calculated for the HiSPARC stations suggest that they should be able to observe higher energy SCRs, but may not be as susceptible as the higher latitude NMs where the effects of GLEs are highly observable.

1.4 HiSPARC Observations

[discuss preliminary observation of space weather FDs and GLEs for the events and singles data...]

[end with discussion on unknown PCRs observable and the effect of atmospheric weather conditions that need to be accounted for]

The effects of space weather on CRs has been outlined in [REF intro]. It was highlighted during communication with the UK Met Office that observations of GLEs are of more interest and importance to space weather forecasts and nowcasts. FDs are of lower interest and importance, however they were still searched for within the HiSPARC data. The events that were looked for within the HiSPARC data are outlined in Table 1.2.

1.4.1 HiSPARC Observations of Ground Level Enhancements

Initial searches for evidence of GLEs within the HiSPARC data were conducted for GLE 70, 71, and 72, as they are the only GLEs that span the operational epoch of

Table 1.2: Space weather events investigated within the HiSPARC data. The percentage change column provides a reference of how much the CR counts observed by the NM station at Oulu ($R_c=0.81$ GV) increased or decreased by, due to the space weather event.

GLE Onset	GLE	% Change (Oulu)	FD Onset	% Change (Oulu)
13/12/2006	70	~ 100%	08/03/2012	~ 5%
17/05/2012	71	~ 15%	14/07/2012	~ 3%
10/09/2017	72	~ 5%	21/12/2014	~ 5%
			06/09/2017	~ 2%
			07/09/2017	~ 8%

the HiSPARC network.

Figure 1.2...

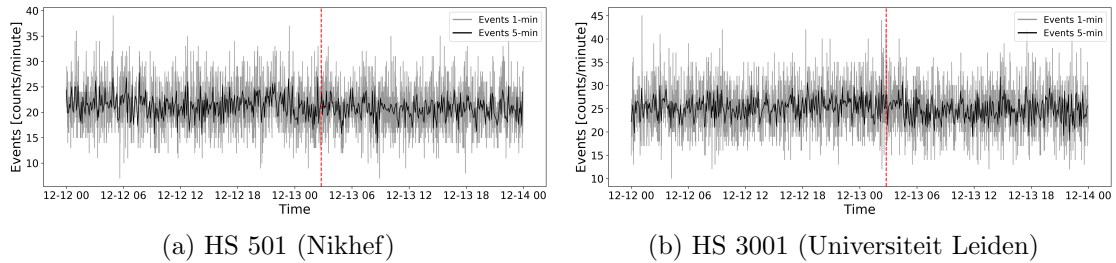


Figure 1.2: HiSPARC data for stations 501 and 3001 around the epoch of GLE 70. The plot shows the minute-averaged and 5-minute-averaged trigger events between detectors within the station. The vertical red, dashed line depicts the approximate onset time of the GLE.

Figure 1.3...

Figure 1.4...

... no clear GLE seen...

1.4.2 HiSPARC Observations of Forbush Decreases

Figure 1.5...

Figure 1.6...

Figure 1.7...

Figure 1.8...

... no clear FDs seen...

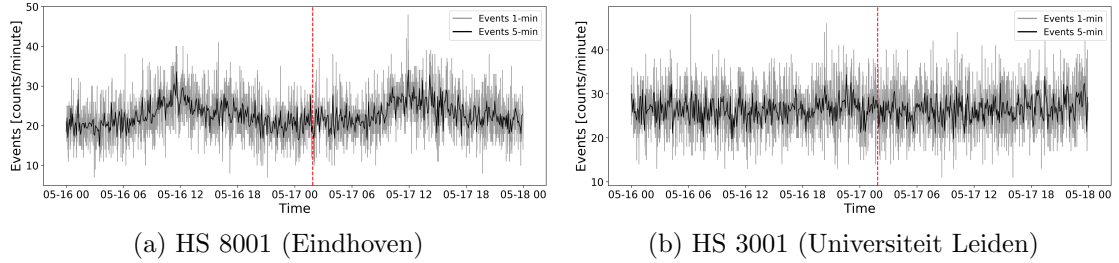


Figure 1.3: HiSPARC data for stations 8001 and 3001 around the epoch of GLE 71. The plot shows the minute-averaged and 5-minute-averaged trigger events between detectors within the station. The vertical red, dashed line depicts the approximate onset time of the GLE.

1.5 Air Shower Simulations

In order to understand the footprint of air showers produced by PCRs, simulations of air showers were performed for a range of primary proton and α -particle energies.

To simulate the CR air shower development, we employ CORSIKA (**C**Osmic **R**ay **S**Imulations for **K**Ascade), a Monte Carlo programme providing detailed simulations of the evolution of air showers initiated by cosmic rays particles through the atmosphere (Heck & Pierog, 2017). The particles in the CORSIKA simulations are tracked through the atmosphere until they undergo interactions with atmospheric nuclei, decay due to their instability, or reach the ground level defined as the end of the simulation.

Proton and α -particle initiated air showers were generated with energies ranging from 10^9 to 10^{20} eV, and 4×10^9 to 10^{20} eV, respectively. In total ~ 230000 proton-initiated showers were simulated and ~ 180000 α -particle-initiated air showers were simulated. The list of simulated air shower PCRs is shown in Table 1.3. For high energy, inelastic hadronic interactions within CORSIKA the QGSJET-II [REF] model was selected. Interactions of hadrons with energies below 80 GeV are simulated using GHEISHA [REF], which allowed for the simulation of PCRs in the regime of SCRs. In addition to these hadronic interactions, electromagnetic interactions within the CORSIKA simulations were described by the EGS4 [REF] model.

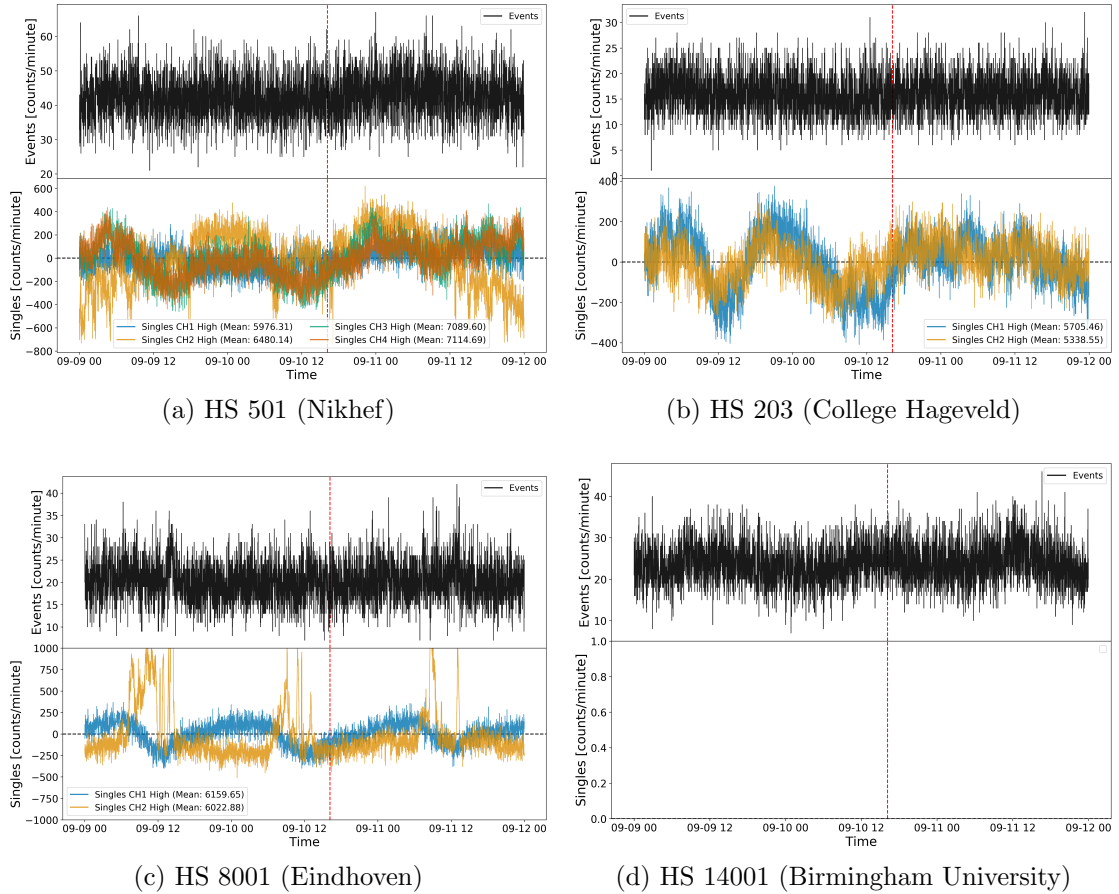


Figure 1.4: HiSPARC data for 4 stations around the epoch of GLE 72. The top panel of each subplot shows the minute-averaged trigger events between detectors within the station, while the bottom panel shows the mean-shifted, minute-averaged counts by each individual detector in the station. The vertical red, dashed line depicts the approximate onset time of the GLE.

Furthermore CORSIKA has a minimum muon energy limit that can be simulated of 10 MeV.

There are several other user-definable setting within CORSIKA which are explained in-depth in the CORSIKA user's guide (Heck & Pierog, 2017). The settings chosen within these simulation are briefly discussed below. Simulation thinning was enable in CORSIKA to reduce computation time and reduce the output file size. The observation level at which point the simulation cease was set at 100 m above sea level (compared to the ~ 50 m typical of the stations, however this difference is negligible for the air shower development.) The pre-defined central European atmosphere in October was used for all simulations, and western-European magnetic

Table 1.3: PCRs simulated using CORSIKA.

Protons				α -Particles			
E _{PCR} (eV)	N _{sims}						
1.00E+09	10000	2.98E+12	1000	4.00E+09	10000	1.00E+13	1000
1.27E+09	10000	3.79E+12	1000	4.28E+09	10000	1.78E+13	100
1.62E+09	10000	4.83E+12	1000	5.46E+09	10000	3.16E+13	100
2.07E+09	10000	6.16E+12	1000	6.95E+09	10000	5.62E+13	100
2.64E+09	10000	7.85E+12	1000	8.86E+09	10000	1.00E+14	100
3.36E+09	10000	1.00E+13	1000	1.00E+10	10000	1.78E+14	50
4.28E+09	10000	1.78E+13	100	1.13E+10	10000	3.16E+14	50
5.46E+09	10000	3.16E+13	100	1.44E+10	10000	5.62E+14	50
6.95E+09	10000	5.62E+13	100	1.83E+10	10000	1.00E+15	10
8.86E+09	10000	1.00E+14	100	2.34E+10	10000	1.78E+15	10
1.00E+10	10000	1.78E+14	50	2.98E+10	10000	3.16E+15	10
1.13E+10	10000	3.16E+14	50	3.79E+10	10000	5.62E+15	10
1.44E+10	10000	5.62E+14	50	4.83E+10	10000	1.00E+16	10
1.83E+10	10000	1.00E+15	10	6.16E+10	10000	1.78E+16	10
2.34E+10	10000	1.78E+15	10	7.85E+10	10000	3.16E+16	10
2.98E+10	10000	3.16E+15	10	1.00E+11	10000	5.62E+16	10
3.79E+10	10000	5.62E+15	10	1.27E+11	1000	1.00E+17	10
4.83E+10	10000	1.00E+16	10	1.62E+11	1000	1.78E+17	10
6.16E+10	10000	1.78E+16	10	2.07E+11	1000	3.16E+17	10
7.85E+10	10000	3.16E+16	10	2.64E+11	1000	5.62E+17	10
1.00E+11	10000	5.62E+16	10	3.36E+11	1000	1.00E+18	10
1.27E+11	1000	1.00E+17	10	4.28E+11	1000	1.78E+18	10
1.62E+11	1000	1.78E+17	10	5.46E+11	1000	3.16E+18	10
2.07E+11	1000	3.16E+17	10	6.95E+11	1000	5.62E+18	10
2.64E+11	1000	5.62E+17	10	8.86E+11	1000	1.00E+19	10
3.36E+11	1000	1.00E+18	10	1.13E+12	1000	1.78E+19	10
4.28E+11	1000	1.78E+18	10	1.44E+12	1000	3.16E+19	10
5.46E+11	1000	3.16E+18	10	1.83E+12	1000	5.62E+19	10
6.95E+11	1000	5.62E+18	10	2.34E+12	1000	1.00E+20	10
8.86E+11	1000	1.00E+19	10	2.98E+12	1000		
1.13E+12	1000	1.78E+19	10	3.79E+12	1000		
1.44E+12	1000	3.16E+19	10	4.83E+12	1000		
1.83E+12	1000	5.62E+19	10	6.16E+12	1000		
2.34E+12	1000	1.00E+20	10	7.85E+12	1000		

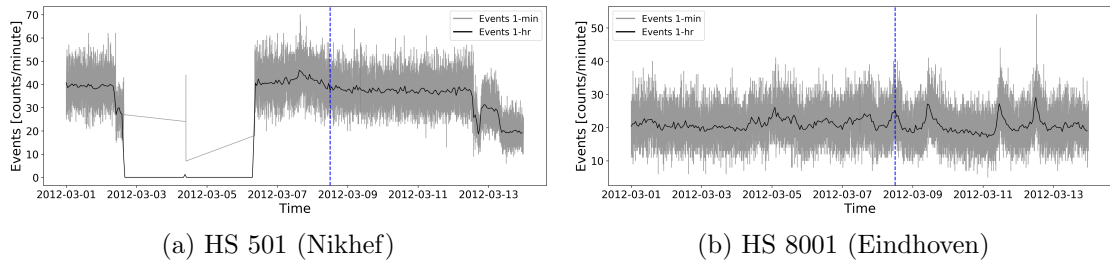


Figure 1.5: HiSPARC data for stations 501 and 8001 around the epoch of the FD in March 2012. The plot shows the minute-averaged and hourly-averaged trigger events between detectors within the station. The vertical blue-dashed line shows the approximate onset-time of the FD.

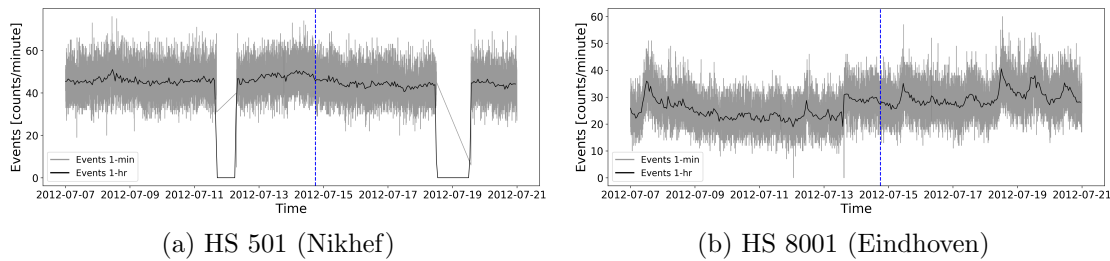


Figure 1.6: HiSPARC data for stations 501 and 8001 around the epoch of the FD in July 2012. The plot shows the minute-averaged and hourly-averaged trigger events between detectors within the station. The vertical blue-dashed line shows the approximate onset-time of the FD.

field was used as calculated with the *Geomag* programme [REF]: $B_x = 18.799 \mu\text{T}$ and $B_z = 44.980 \mu\text{T}$.

1.5.1 Air Shower Footprints

The average footprint of muons at ground level was acquired from the output CORSIKA simulations. This was achieved by simply taking the distribution of the muons at ground level at the end of the simulation as a function of their distance from the shower core for each individual simulation realisation. For a given PCR energy the average air shower footprint distribution is calculated by combining the individual simulation realisations.

The interpretation of Figure 1.9 can provide an understanding of the minimum energy of PCRs observable by the different stations within the HiSPARC network. The typical separation between the detectors in a HiSPARC station is $\sim 10 \text{ m}$,

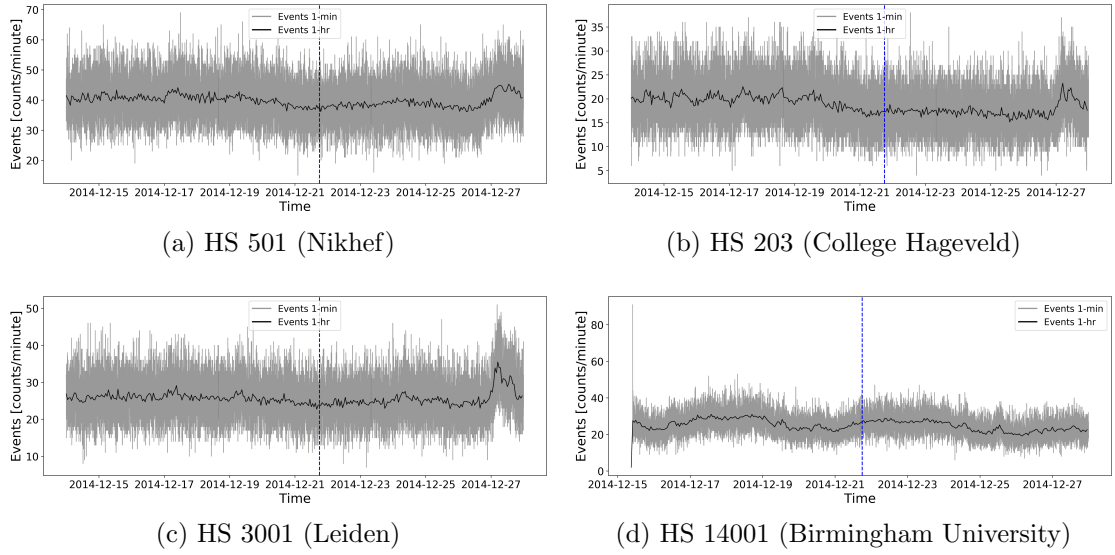


Figure 1.7: HiSPARC data for 4 stations around the epoch of the FD in December 2014. The plot shows the minute-averaged and hourly-averaged trigger events between detectors within the station. The vertical blue-dashed line shows the approximate onset-time of the FD.

however the separation between detectors can be up to as much as 20 m or as low as a couple of metres. This analysis of the air shower footprint shows the variation in PCR energy sampled varies marginally over this range of distances and suggests that HiSPARC stations will typically observe PCR with an energy of $\sim 10^{14} - 10^{15}$ eV to meet the required trigger conditions.

1.5.2 Muon Flux

From the air shower simulations it is possible to gain an estimate of the muon flux at ground-level based on the number of

1.6 Standardisation of HiSPARC Data

1.6.1 Motivation

1.6.2 Barometric Correction

It is understood that observations made by ground-based CR detectors are susceptible to atmospheric conditions. Atmospheric pressure effects the CR travel path due

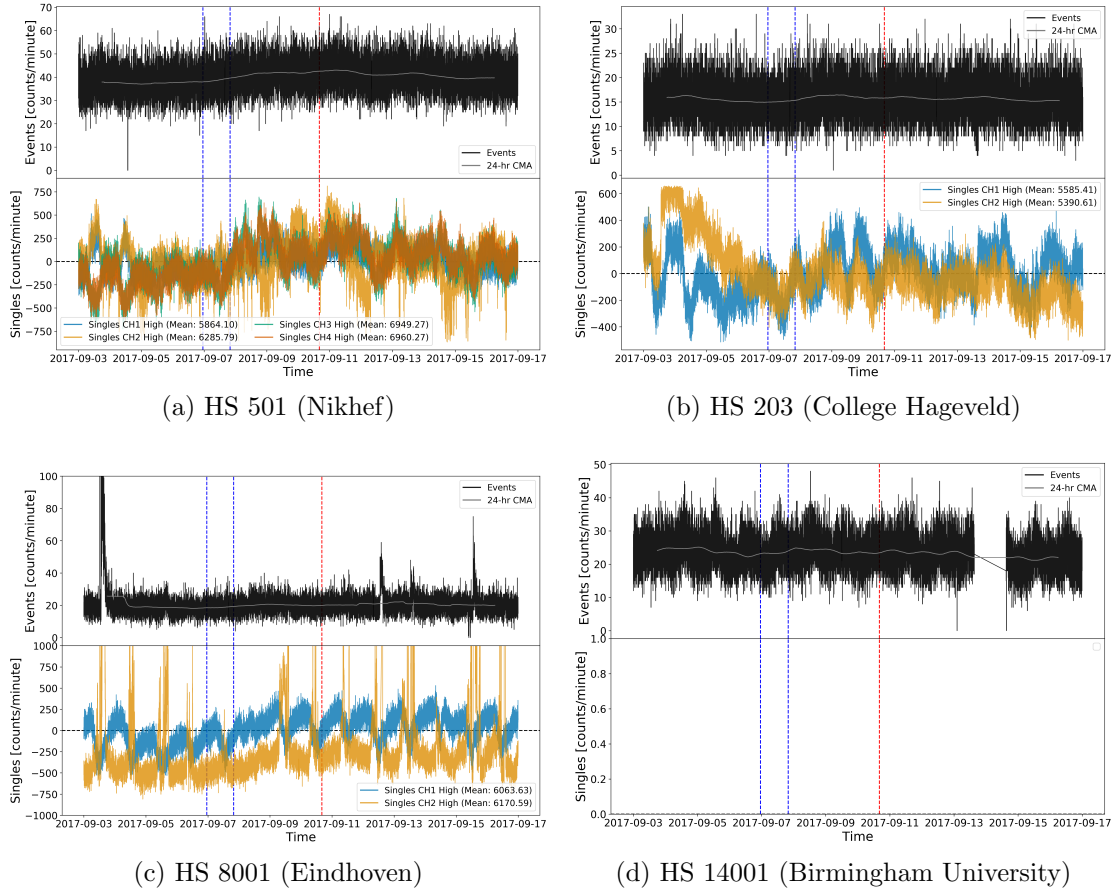
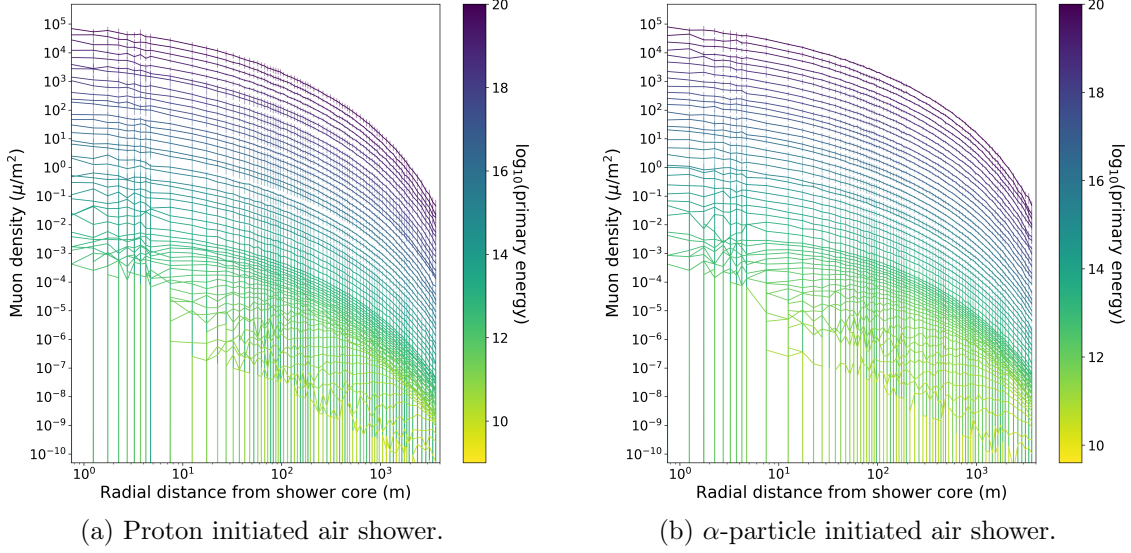


Figure 1.8: HiSPARC data for [n] stations around the epoch in which there were several FDs close to the onset of GLE 72. The top panel of each subplot shows the minute-averaged trigger events between detectors within the station, while the bottom panel shows the mean-shifted, minute-averaged counts by each individual detector in the station. The vertical blue-dashed lines show the approximate onset-times of the two FDs observed around this epoch and the red-dashed line depicts the approximate onset time of the GLE.

to the expansion and contraction of the atmosphere with varying pressure; hence the CR counts are observed to be negatively correlated to atmospheric pressure [add example plot to show].

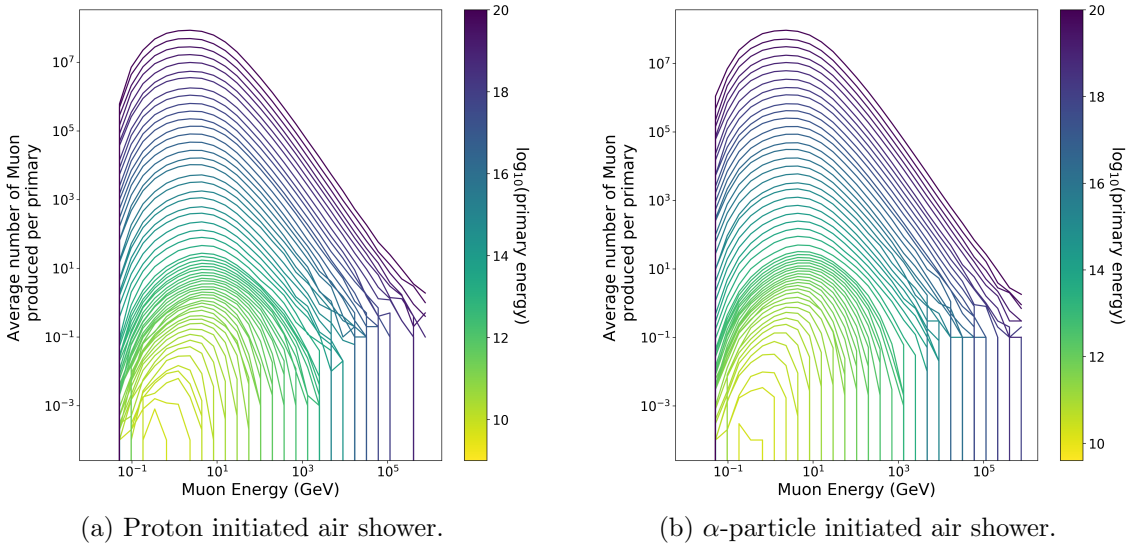
The method of correcting for the barometric effect is discussed widely in the neutron monitor literature and is shown to depend on the barometric coefficient. If the cosmic ray flux is constant, N , CR variations depend on the local atmospheric pressure as described by equation (1.1), where ΔN is the change in count rate, β is the barometric coefficient, and $\Delta P = P - P_0$ is the deviation in pressure from the average (P_0) in the given time-period (Paschalis et al., 2013):



(a) Proton initiated air shower.

(b) α -particle initiated air shower.

Figure 1.9: Mean muon density footprints for (a) proton-initiated air showers and (b) α -particle-initiated air showers with intial PCR trajectories with zenith angles $\theta = 0^\circ$ and various PCR energies. The error bars given represent 1σ .



(a) Proton initiated air shower.

(b) α -particle initiated air shower.

Figure 1.10: Mean number of muons produced at ground level by the PCR for (a) proton-initiated air showers and (b) α -particle-initiated air showers, for various PCR energy. The uncertainty bars given represent 1σ .

$$\Delta N = -\beta N \Delta P \quad (1.1)$$

Through the integration of equation (1.1), the solution shows the dependence of cosmic ray intensity on pressure as in equation (1.2).

$$N = N_0 e^{-\beta \Delta P} \quad (1.2)$$

Therefore by taking the natural logarithm of equation (1.2), one can obtain the barometric coefficient through fitting the straight line in equation (1.3) to the observed data, where N_0 may be assumed as the average count rate over the given time-period.

$$\ln \left(\frac{\Delta N}{N} \right) = -\beta \Delta P \quad (1.3)$$

1.6.3 Temperature Correction

2 HiSPARC Station 14008

2.1 Introduction

2.2 Aims

2.3 HiSPARC 14008 Detector Set-up

2.4 Calibration

2.5 Observations

2.6 Observations

2.7 Conclusions

Bibliography

Heck D., Pierog T., 2017, Technical Report 7.6400, Extensive Air Shower Simulation with CORSIKA: A Users Guide

Paschalis P., Mavromichalaki H., Yanke V., Belov A., Eroshenko E., Gerontidou M., Koutroumpi I., 2013, New Astronomy, 19, 10